

## QUANTUM CHEMICAL DESCRIPTORS OF SOME *P*-AMINOPHENYL TETRATHIAFULVALENES THROUGH DENSITY FUNCTIONAL THEORY (DFT)

A. Bendjeddou<sup>1,\*</sup>, T. Abbaz<sup>1,3</sup>, S. Maache<sup>1</sup>, R. Rehamnia<sup>2</sup>, A. K. Gouasmia<sup>3</sup>  
and D. Villemin<sup>4</sup>

<sup>1</sup>Laboratory of Aquatic and Terrestrial Ecosystems, Organic and Bioorganic Chemistry Group, University of Mohamed-Cherif Messaadia, Souk Ahras, Algeria

<sup>2</sup>Chemistry Department, Faculty of Science, University of badji mokhtar, Annaba, Algeria

<sup>3</sup>Laboratory of Organic Materials and Heterochemistry, University of Larbi Tebessi, Tebessa, Algeria

<sup>4</sup>Laboratory of Molecular and Thio-Organic Chemistry, UMR CNRS 6507, INC3M, FR 3038, Labex EMC3, ensicaen & University of Caen, Caen 14050, France

\*E-mail : amel.bendjeddou@univ-soukahras.dz

### ABSTRACT

In this work we have been calculated global and local DFT reactivity descriptors for some *p*-aminophenyl tetrathiafulvalenes such as: the ionization potential (I), electron affinity (A), electronegativity ( $\chi$ ), electrophilicity ( $\omega$ ), and hardness ( $\eta$ ) have been calculated using density functional theory (DFT) approach with B3LYP/6-31G(d,p) level of theory. The plots of frontier molecular orbital and molecular electrostatic potential (MESP) have been demonstrated. The chemometric methods PCA and HCA were employed to find the subset of variables that could correctly classify the compounds according to their reactivity.

**Keywords:** Tetrathiafulvalenes, Density functional theory, Reactivity descriptors, Principal component analysis and Hierarchical cluster analysis.

©2016 RASĀYAN. All rights reserved

### INTRODUCTION

During the last decades, density functional theory (DFT) has undergone fast development, especially in the field of organic chemistry<sup>1,2</sup>, as the number of accurate exchange-correlation functionals increased. Indeed, the apparition of gradient corrected and hybrid functionals in the late 1980s greatly improved the chemical accuracy of the Hohenberg-Kohn theorem based methods<sup>3</sup>. The Kohn-Sham formalism and its density-derived orbitals paved the way to computational methods. In parallel, a new field of application of DFT developed, the so-called conceptual DFT<sup>4,5</sup>. Density functional methodology has been found to be very constructive in explaining the chemical reactivity, stability and site selectivity of molecular systems which makes use of the quantum molecular descriptors like chemical potential, global hardness, softness, electrophilicity etc. These descriptors have been tested and studied in the literature by several research groups and are found to be very useful in rationalizing the reactivity patterns of the molecular systems<sup>6-11</sup>.

Geerlings et al. along with Roy and co-workers have reviewed and tested the theoretical basis for these descriptors and their applications<sup>12,13</sup>. Chattaraj et al. also have recently reviewed the theoretical basis for these descriptors and their applications in various molecular systems<sup>14</sup>. In general, the descriptors are classified as global and local reactivity descriptors. Since most of these descriptors are the derivatives of energy and electron density variables, it is expected that they will provide the modified reactivity information of the molecular systems<sup>15,16</sup>.

Moreover, starting from the work of Fukui and its frontier molecular orbitals (FMOs) theory<sup>17</sup>, the same authors further generalized the concept and proposed the Fukui function  $f(r)$  as a tool for describing the local reactivity in molecules<sup>18,19</sup>. Therefore, in this study, the objective of this work is to perform a detailed calculation of the molecular structure and chemical reactivity of some *p*-aminophenyl tetrathiafulvalenes.

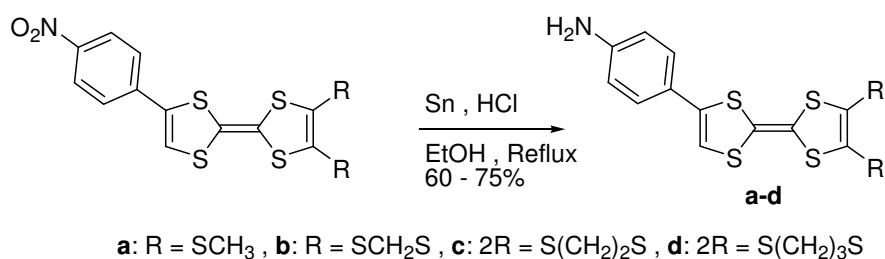
## EXPERIMENTAL

## Material and Methods

All computational calculations have been performed on personal computer using the Gaussian 09W program packages developed by Frisch and coworkers<sup>20</sup>. The Becke's three parameter hybrid functional using the LYP correlation functional (B3LYP), one of the most robust functional of the hybrid family, was herein used for all the calculations, with 6.31G (d, p) basis set<sup>21,22</sup>. Gaussian output files were visualized by means of GAUSSIAN VIEW 05 software<sup>23</sup>. Principal component analysis (PCA) and Hierarchical cluster analysis (HCA) are two chemometric methods were performed using software XLSTAT<sup>24,25</sup>.

## RESULTS AND DISCUSSION

In a previous work<sup>26</sup>, we have described the synthesis of new unsymmetrical tetrathiafulvalenes (TTF) containing aminophenyl rings (**a-d**) indicated in Scheme-1. The synthesis of these electron donors was carried out using the conversion of the nitro moiety to amino group's using reduction reaction.



Scheme-1: Synthetic route for the preparation of *p*-aminophenyl tetrathiafulvalènes (**a-d**)

## Molecular geometry

The structure of a molecule contains the features responsible for its physical, chemical, and biological properties, and that variations in the fate within a series of similar structures can be correlated with changes in descriptors that reflect their molecular properties. The molecular geometry analysis plays a very important role in determining the structure-activity relationship<sup>27</sup>. The molecular geometry can be described by the positions of atoms in space, evoking bond lengths of two joined atoms, bond angles of three connected atoms, and torsion angles (dihedral angles) of three consecutive bonds. The molecular geometries can be determined by the quantum mechanical behavior of the electrons and computed by *ab-initio* quantum chemistry methods to high accuracy. Molecular geometry represents the three dimensional arrangement of the atoms that determines several properties of a substance including its reactivity, polarity, phase of matter, color, magnetism, and biological activity<sup>28,29</sup>. The optimization of the geometry for the molecules (**a-d**) has been achieved by energy minimization, using DFT at the B3LYP level, employing the basis set 6-31G (d,p). The following Fig.-1, Table-1 and Table-2 represent the schemes of the optimized molecules, their bond lengths and their angle measurement.

Table-1: Optimized geometric parameters of compound (**a**) and (**b**)

Compound (a)				Compound (b)			
Bond length(Å)		Angles(°)		Bond length(Å)		Angles(°)	
C <sub>3</sub> C <sub>5</sub>	1.345	S <sub>4</sub> C <sub>3</sub> S <sub>2</sub>	113.686	C <sub>4</sub> C <sub>3</sub>	1.350	S <sub>10</sub> C <sub>1</sub> S <sub>9</sub>	124.260
S <sub>4</sub> C <sub>3</sub>	1.783	S <sub>6</sub> C <sub>7</sub> S <sub>12</sub>	117.609	C <sub>1</sub> S <sub>9</sub>	1.774	C <sub>4</sub> C <sub>3</sub> S <sub>10</sub>	123.290
S <sub>9</sub> C <sub>8</sub>	1.790	S <sub>4</sub> C <sub>1</sub> C <sub>10</sub>	119.604	C <sub>3</sub> S <sub>10</sub>	1.791	S <sub>9</sub> C <sub>1</sub> C <sub>10</sub>	124.260
C <sub>8</sub> S <sub>13</sub>	1.766	C <sub>3</sub> S <sub>4</sub> C <sub>10</sub>	94.933	C <sub>4</sub> C <sub>13</sub>	1.778	C <sub>4</sub> S <sub>13</sub> C <sub>6</sub>	95.451
C <sub>7</sub> S <sub>12</sub>	1.766	S <sub>13</sub> C <sub>8</sub> C <sub>7</sub>	125.538	C <sub>6</sub> C <sub>14</sub>	1.470	C <sub>2</sub> S <sub>8</sub> C <sub>27</sub>	91.474
C <sub>10</sub> C <sub>22</sub>	1.471	C <sub>7</sub> S <sub>12</sub> C <sub>14</sub>	101.759	C <sub>14</sub> C <sub>15</sub>	1.406	S <sub>13</sub> C <sub>6</sub> C <sub>14</sub>	118.023
C <sub>22</sub> C <sub>23</sub>	1.406	C <sub>1</sub> C <sub>10</sub> C <sub>22</sub>	126.318	C <sub>21</sub> N <sub>24</sub>	1.390	C <sub>5</sub> C <sub>6</sub> C <sub>14</sub>	126.681
C <sub>29</sub> N <sub>32</sub>	1.391	C <sub>25</sub> C <sub>29</sub> N <sub>32</sub>	120.953	C <sub>16</sub> C <sub>19</sub>	1.387	C <sub>14</sub> C <sub>16</sub> C <sub>19</sub>	121.431
S <sub>13</sub> C <sub>18</sub>	1.837	C <sub>24</sub> C <sub>22</sub> C <sub>23</sub>	117.488	C <sub>27</sub> H <sub>28</sub>	1.092	C <sub>17</sub> C <sub>21</sub> C <sub>19</sub>	118.151
N <sub>32</sub> H <sub>34</sub>	1.010	C <sub>22</sub> C <sub>23</sub> C <sub>25</sub>	121.419	N <sub>24</sub> H <sub>26</sub>	1.010	C <sub>19</sub> C <sub>21</sub> N <sub>24</sub>	120.814

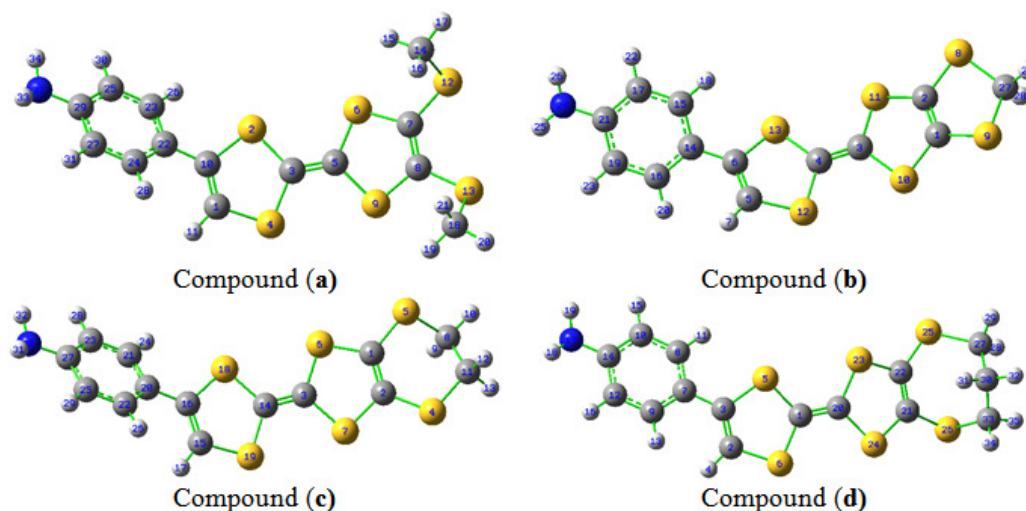


Fig.-1: Optimized molecular structure of the minimum energy structure of *p*-Aminophenyl tetrathiafulvalenes obtained at B3LYP/6-31G(d,p) level

Table-2: Optimized geometric parameters of compound (c) and (d)

Compound (c)				Compound (d)			
Bond length(Å)		Angles(°)		Bond length(Å)		Angles(°)	
C <sub>3</sub> S <sub>6</sub>	1.782	C <sub>3</sub> S <sub>6</sub> C <sub>1</sub>	93.410	C <sub>1</sub> C <sub>5</sub>	1.780	C <sub>2</sub> C <sub>3</sub> C <sub>7</sub>	126.602
C <sub>1</sub> S <sub>5</sub>	1.763	C <sub>1</sub> S <sub>5</sub> C <sub>8</sub>	96.414	C <sub>3</sub> C <sub>7</sub>	1.470	C <sub>5</sub> C <sub>3</sub> C <sub>7</sub>	118.089
S <sub>4</sub> C <sub>11</sub>	1.862	C <sub>7</sub> C <sub>2</sub> C <sub>1</sub>	116.700	C <sub>7</sub> C <sub>9</sub>	1.407	C <sub>3</sub> C <sub>7</sub> C <sub>9</sub>	120.803
C <sub>8</sub> C <sub>11</sub>	1.521	C <sub>14</sub> C <sub>3</sub> S <sub>7</sub>	123.583	C <sub>1</sub> C <sub>20</sub>	1.350	C <sub>20</sub> C <sub>1</sub> S <sub>5</sub>	123.451
C <sub>3</sub> C <sub>14</sub>	1.351	C <sub>2</sub> S <sub>4</sub> C <sub>11</sub>	103.849	C <sub>8</sub> C <sub>10</sub>	1.389	C <sub>7</sub> C <sub>9</sub> C <sub>12</sub>	121.442
S <sub>18</sub> C <sub>16</sub>	1.788	C <sub>14</sub> S <sub>19</sub> C <sub>15</sub>	94.915	C <sub>14</sub> N <sub>17</sub>	1.391	S <sub>24</sub> C <sub>21</sub> S <sub>26</sub>	118.620
C <sub>16</sub> C <sub>20</sub>	1.471	C <sub>16</sub> S <sub>18</sub> C <sub>14</sub>	95.822	C <sub>21</sub> S <sub>26</sub>	1.766	C <sub>10</sub> C <sub>14</sub> C <sub>12</sub>	118.155
C <sub>22</sub> C <sub>20</sub>	1.406	S <sub>19</sub> C <sub>15</sub> C <sub>16</sub>	119.571	S <sub>26</sub> C <sub>33</sub>	1.852	C <sub>10</sub> C <sub>14</sub> N <sub>17</sub>	120.942
C <sub>25</sub> C <sub>22</sub>	1.388	C <sub>15</sub> C <sub>16</sub> S <sub>18</sub>	115.416	C <sub>30</sub> C <sub>27</sub>	1.531	S <sub>25</sub> C <sub>22</sub> C <sub>21</sub>	127.806
C <sub>27</sub> N <sub>30</sub>	1.391	C <sub>15</sub> C <sub>16</sub> C <sub>20</sub>	126.305	C <sub>33</sub> H <sub>34</sub>	1.093	S <sub>26</sub> C <sub>21</sub> C <sub>22</sub>	124.468

### Molecular electrostatic potential (ESP) map

Electrostatic potential maps, also known as electrostatic potential energy maps, or molecular electrical potential surfaces, illustrate the charge distributions of molecules three dimensionally. The purpose of finding the electrostatic potential is to find the reactive site of a molecule. These maps allow us to visualize variably charged regions of a molecule. Knowledge of the charge distributions can be used to determine how molecules interact with one another. Molecular electrostatic potential (MESP) mapping is very useful in the investigation of the molecular structure with its physiochemical property relationships<sup>30</sup>. Total SCF electron density surface mapped with molecular electrostatic potential (MESP) of compounds (a) and (c) are shown in Fig.-2.

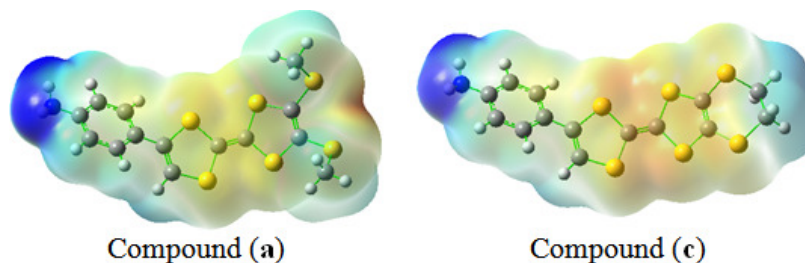


Fig.-2: Molecular electrostatic potential surface of compounds (a) and (c)

The negative electrostatic potential corresponds to an attraction of the proton by the concentrated electron density in the molecule (red color on the ESP surface), whereas the positive electrostatic potential corresponds to repulsion of the proton by atomic nuclei in regions where low electron density exists and the nuclear charge is incompletely shielded (blue color on the ESP surface). Electrostatic potential increases in the order red < orange < yellow < green < blue. The ESP surface has three projections, one in molecular plane and two in perpendicular planes. ESP provides a visual method to understand the relative polarity of a molecule. It also serves as a useful quantity to explain electronegativity, partial charges, site of chemical reactivity, structure-activity relationship, hydrogen bonding and other interactions of molecules including biomolecules and drugs.

### Global reactivity descriptors

The values of the calculated quantum chemical parameters such as the energy of the highest occupied molecular orbital ( $E_{\text{HOMO}}$ ), energy of the lowest unoccupied molecular orbital ( $E_{\text{LUMO}}$ ), energy gap ( $\Delta E_{\text{gap}}$ ), ionization energy (I), electron affinity (A) are presented in Table-3. Frontier molecular orbitals (FMOs), HOMO and LUMO plot of compound (a) are shown in Fig.-3. The highest occupied molecular orbital (HOMO) and lowest unoccupied molecular orbital (LUMO) are very popular quantum chemical parameters. The FMOs are important in determining molecular reactivity and the ability of a molecule to absorb light. The vicinal orbitals of HOMO and LUMO play the same role of electron donor and electron acceptor respectively. The energies of HOMO and LUMO and their neighboring orbitals are all negative, which indicate the title molecule is stable<sup>31</sup>. The HOMO-LUMO energy gap ( $\Delta E_{\text{gap}}$ ) is an important stability index. The HOMO-LUMO energy gap of title molecule reflects the chemical stability of the molecule. Through Koopman's theorem<sup>32</sup>, the HOMO and LUMO energy values are related to the ionization potential ( $I = -E_{\text{HOMO}}$ ) and electron affinities ( $A = -E_{\text{LUMO}}$ ). (I) and (A) are calculated as the negative of energy eigen-values of HOMO and LUMO respectively.

Table-3: Energetic parameters of *p*-Aminophenyl tetrathiafulvalenes (a-d)

Compounds	$E_{\text{HOMO}}$ (eV)	$E_{\text{LUMO}}$ (eV)	$\Delta E_{\text{gap}}$ (eV)	I (eV)	A (eV)
a	-4.580	-0.961	3.619	4.580	0.961
b	-4.590	-0.994	3.596	4.590	0.994
c	-4.515	-0.945	3.570	4.515	0.945
d	-4.522	-0.897	3.626	4.522	0.897

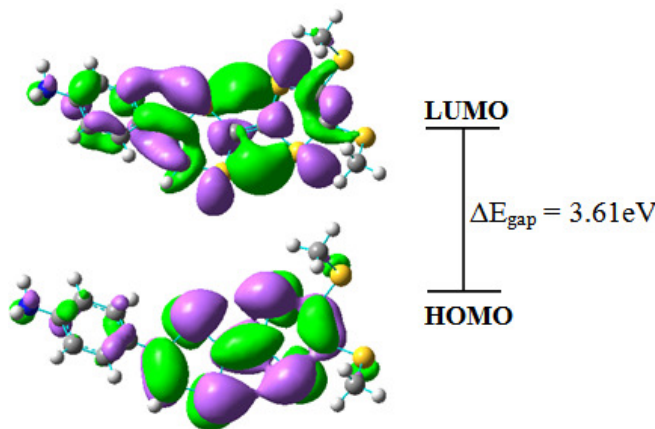


Fig.-3: Highest occupied molecular orbitals and lowest unoccupied molecular orbitals of (a)

Several calculated electronic parameters are listed in Table-4. These parameters are used to describe chemical reactivity of molecules. The electronic parameters chemical potential ( $\mu$ ), absolute electro negativity ( $\chi$ ) and chemical hardness ( $\eta$ ), global softness (S) and electrophilicity ( $\omega$ ) are calculated at B3LYP/6-31G (d,p) level.

Electronegativity ( $\chi$ ) is related to the electron donating properties of molecule and is the negative of the chemical potential ( $\mu$ ) in Mulliken sense<sup>33</sup>. The global hardness ( $\eta$ ), and chemical potential ( $\mu$ ) is defined as the second and first derivative of the energy ( $E$ ), with respect to the number of electrons ( $N$ ), at constant external potential  $\bar{v}(r)$ , captures the resistance of a chemical species to changing its electronic number<sup>34-37</sup>. Parr defined the electrophilicity index ( $\omega$ ), as a numerical value which is related to the stabilization of energy when the system acquires an electronic charge and serves as an indicator of the reactivity of a system towards nucleophiles<sup>38</sup>. Softness ( $S$ ) is a property of molecules that measures the extent of chemical reactivity; it is the reciprocal of hardness.

Table-4: Quantum chemical descriptors of *p*-Aminophenyl tetrathiafulvalenes (**a-d**)

Compounds	$\mu$ (eV)	$\chi$ (eV)	$\eta$ (eV)	$S$ (eV)	$\omega$ (eV)
a	-2.771	2.775	1.810	0.276	2.121
b	-2.792	2.792	1.798	0.278	2.168
c	-2.730	2.730	1.785	0.280	2.088
d	-2.710	2.710	1.813	0.276	2.025

According to these parameters, the chemical reactivity varies with the structural of molecules. Chemical hardness (softness) value of compound (**c**) is lesser (greater) among all the molecules. Thus, compound (**c**) is found to be more reactive than all the molecules. Compound (**b**) possesses higher electronegativity value than all compounds so; it is the best electron acceptor. The values of  $\omega$  for compounds (**a-d**) indicate that they are two series (**a, b**) and (**c, d**). The first one has the high value of electrophilicity index which, shows that the compounds of this group are a strong electrophiles.

### Local reactivity descriptors

Local reactivity descriptors are used to decide relative reactivity of different atoms in the molecule. It is established that molecule tends to react where the value of descriptor is largest when attacked by soft reagent and where the value is smaller when attacked by hard reagent<sup>39</sup>. The use of descriptors for the site selectivity of the molecule for nucleophilic and electrophilic attack has been made.

Fukui functions  $f^+(r)$ ,  $f^-(r)$  and  $f^0(r)$  are calculated using the following equations as<sup>40-43</sup>:

$$f^+ = [q(N+1) - q(N)], \text{ for nucleophilic attack,}$$

$$f^- = [q(N) - q(N-1)], \text{ for electrophilic attack,}$$

$$f^0 = [q(N+1) - q(N-1)]/2, \text{ for radical attack.}$$

Where  $q(N)$  is the charge on  $k$ th atom for neutral molecule while  $q(N+1)$  and  $q(N-1)$  are the same for its anionic and cationic species, respectively. The value of descriptors calculated at B3LYP/6-31G (d,p) level using Mulliken charges on atoms in molecules are presented in Tables-5 and 6.

Table-5: Values of the Fukui function considering NBO charges of the molecules (**a**) and (**b**)

Compound (a)				Compound (b)			
Atom	$f^+$	$f^-$	$f^0$	Atom	$f^+$	$f^-$	$f^0$
1 C	-0.291	0.058	-0.116	1 C	-0.300	0.095	-0.106
2 S	0.164	-0.247	-0.041	2 C	-0.313	0.095	-0.109
3 C	-0.238	0.091	-0.073	3 C	-0.287	0.037	-0.125
4 S	0.183	-0.249	-0.032	4 C	-0.232	0.082	-0.075
5 C	-0.262	0.022	-0.120	5 C	-0.294	0.060	-0.117
6 S	0.201	-0.222	-0.010	6 C	-0.196	0.039	-0.078
7 C	-0.216	0.104	-0.056	7 H	0.011	-0.104	-0.046
8 C	-0.256	0.070	-0.089	8 S	0.112	-0.166	-0.027
9 S	0.227	-0.210	0.008	9 S	0.102	-0.126	-0.012
10 C	-0.176	0.037	-0.069	10 S	0.287	0.078	0.183
11 H	0.010	-0.102	-0.046	11 S	0.239	-0.218	0.010
12 S	0.117	-0.091	0.013	12 S	0.187	-0.252	-0.032
13 S	0.086	-0.103	-0.008	13 S	0.197	-0.249	-0.026
14 C	0.086	0.027	0.056	14 C	-0.133	<u>0.159</u>	0.013

15 H	-0.043	-0.004	-0.023	15 C	-0.026	-0.007	-0.017
16 H	-0.044	-0.016	-0.030	16 C	-0.027	-0.009	-0.018
17 H	-0.037	-0.040	-0.038	17 C	-0.025	0.073	0.024
18 C	0.098	0.042	0.070	18 H	0.004	-0.071	-0.033
19 H	-0.062	-0.008	-0.035	19 C	-0.036	0.075	0.019
20 H	-0.044	-0.043	-0.044	20 H	0.025	-0.085	-0.030
21 H	-0.042	-0.014	-0.028	21 C	-0.384	-0.042	-0.213
22 C	-0.147	<u>0.164</u>	0.008	22 H	0.018	-0.094	-0.038
23 C	-0.025	-0.009	-0.017	23 H	0.018	-0.095	-0.038
24 C	-0.017	-0.011	-0.014	24 N	<u>0.371</u>	0.102	<u>0.237</u>
25 C	-0.024	0.072	0.024	25 H	-0.126	-0.055	-0.091
26 H	0.003	-0.072	-0.034	26 H	-0.126	-0.054	-0.090
27 C	-0.036	0.073	0.018	27 C	0.044	0.076	0.060
28 H	0.024	-0.086	-0.030	28 H	-0.060	-0.034	-0.047
29 C	-0.389	-0.041	-0.215	29 H	-0.051	-0.048	-0.050
30 H	0.016	-0.093	-0.038				
31 H	0.018	-0.095	-0.038				
32 N	<u>0.372</u>	0.101	<u>0.237</u>				
33 H	-0.127	-0.055	-0.091				
34 H	-0.128	-0.053	-0.090				

Table-6: Values of the Fukui function considering NBO charges of the molecules (c) and (d)

Compound (c)				Compound (d)			
Atom	$f^+$	$f^-$	$f^0$	Atom	$f^+$	$f^-$	$f^0$
1 C	-0.236	0.094	-0.070	1 C	-0.237	0.085	-0.076
2 C	-0.247	0.105	-0.070	2 C	-0.293	0.059	-0.117
3 C	-0.261	0.022	-0.119	3 C	-0.183	0.041	-0.071
4 S	0.091	-0.304	-0.106	4 H	0.011	-0.102	-0.045
5 S	0.104	-0.314	-0.105	5 S	0.181	-0.249	-0.034
6 S	0.227	-0.030	0.098	6 S	0.186	-0.248	-0.031
7 S	0.219	-0.030	0.094	7 C	-0.140	<u>0.158</u>	0.008
8 C	0.046	0.064	0.055	8 C	-0.027	-0.008	-0.017
9 H	-0.048	-0.036	-0.042	9 C	-0.019	-0.009	-0.014
10 H	-0.034	-0.050	-0.042	10 C	-0.024	0.073	0.024
11 C	0.034	0.078	0.056	11 H	0.002	-0.070	-0.033
12 H	-0.043	-0.040	-0.042	12 C	-0.036	0.074	0.018
13 H	-0.036	-0.049	-0.042	13 H	0.024	-0.086	-0.030
14 C	-0.243	0.088	-0.077	14 C	-0.389	-0.039	-0.214
15 C	-0.288	-0.102	-0.195	15 H	0.017	-0.093	-0.037
16 C	-0.181	<u>0.196</u>	0.007	16 H	0.018	-0.095	-0.038
17 H	0.010	-0.102	-0.046	17 N	<u>0.372</u>	0.100	<u>0.236</u>
18 S	0.174	-0.240	-0.033	18 H	-0.127	-0.054	-0.090
19 S	0.171	-0.243	-0.035	19 H	-0.127	-0.052	-0.090
20 C	-0.146	0.164	0.009	20 C	-0.278	0.028	-0.124
21 C	-0.025	-0.009	-0.017	21 C	-0.253	0.087	-0.082
22 C	-0.017	-0.011	-0.014	22 C	-0.207	0.111	-0.048
23 C	-0.025	0.073	0.024	23 S	0.222	-0.213	0.004
24 H	0.005	-0.073	-0.033	24 S	0.215	-0.217	-0.001
25 C	-0.036	0.074	0.019	25 S	0.104	-0.098	0.003
26 H	0.023	-0.085	-0.030	26 S	0.097	-0.117	-0.009
27 C	-0.389	-0.040	-0.214	27 C	0.036	0.089	0.063
28 H	0.017	-0.093	-0.038	28 H	-0.032	-0.043	-0.037
29 H	0.018	-0.095	-0.038	29 H	-0.036	-0.050	-0.043
30 N	<u>0.372</u>	0.101	<u>0.237</u>	30 C	0.043	0.013	0.028
31 H	-0.127	-0.054	-0.090	31 H	-0.034	-0.018	-0.026
32 H	-0.127	-0.054	-0.091	32 H	-0.039	-0.041	-0.040
				33 C	0.030	0.092	0.061
				34 H	-0.043	-0.044	-0.044
				35 H	-0.033	-0.059	-0.046

Parameters of local reactivity descriptors show that nitrogen N is more reactive site for nucleophilic and free radical attacks in compounds (a-d) and the more reactive site for electrophilic attack is 22C for compound (a), 14C for compound (b), 16C for compound (c) and 7C for compound (d).

### Principal Component Analysis (PCA)

In this work, we auto scaled all calculated variables in order to compare them in the same scale. Afterwards, PCA (principal component analysis) was used to reduce the number of variables and select the most relevant ones, i.e. those responsible for the *p*-Aminophenyl tetrathiafulvalenes reactivity. After performing many tests, a good separation is obtained between more active and less active tetrathiafulvalenes compounds using ten variables: I, A,  $\chi$ ,  $\eta$ , s,  $\mu$ ,  $\omega$ ,  $E_{\text{HOMO}}$ ,  $E_{\text{LUMO}}$ ,  $\Delta E_{\text{gap}}$  (see Tables-3 and 4).

We can observe from PCA results that the first three principal components (PC1, PC2 and PC3) describe 99.99% of the overall variance as follows: PC1 = 67.41%, PC2 = 32.40% and PC3 = 0.18%. The score plot of the variances is a reliable representation of the spatial distribution of the points for the data set studied after explaining almost all of the variances by the first two PCs. The most informative score plot is presented in Fig.-4 (PC1 versus PC2) and we can see that PC1 alone is responsible for the separation between more active (a, b) and less active compounds (c, d) where  $PC1 > 0$  for the more active compounds and  $PC1 < 0$  for the less active ones. The same results follow in the case of global reactivity trend based on  $\omega$ .

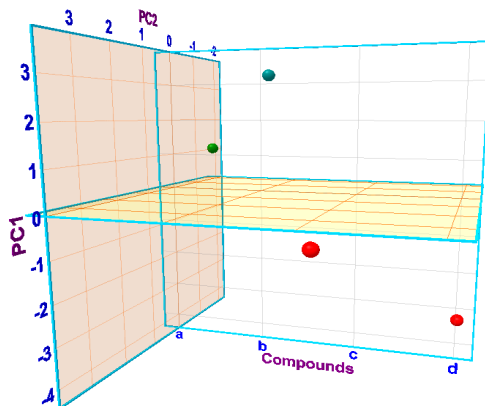


Fig.-4: Score plot for *p*-Aminophenyl tetrathiafulvalenes in gas phase

The loading vectors for the first two principal components (PC1 and PC2) are displayed in Fig.-5. We can see that more active compounds ( $PC1 > 0$ ) can be obtained when we have higher A, I, S,  $\chi$ ,  $\omega$ , values. In this way, some important features on the more active compounds can be observed.

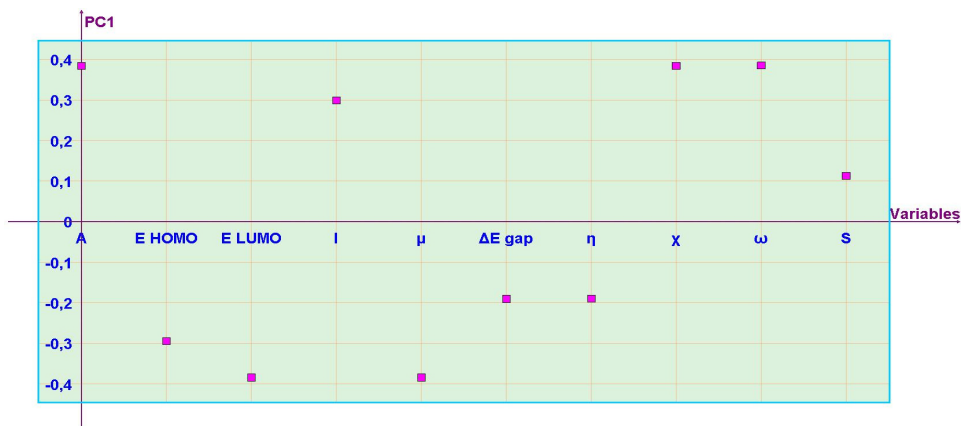


Fig.-5: Loading plot for the variables responsible for the classification of the *p*-Aminophenyl tetrathiafulvalenes studied

### Hierarchical Cluster Analysis (HCA)

Fig.-6 shows HCA analysis of the current study. The horizontal lines represent the compounds and the vertical lines the similarity values between pairs of compounds, a compound and a group of compounds and among groups of compounds. We can note that HCA results are very similar to those obtained with the PCA analysis, i.e. the compounds studied were grouped into two categories: more actives (compounds: (a) and (b)) and less active (compounds: (c) and (d)).

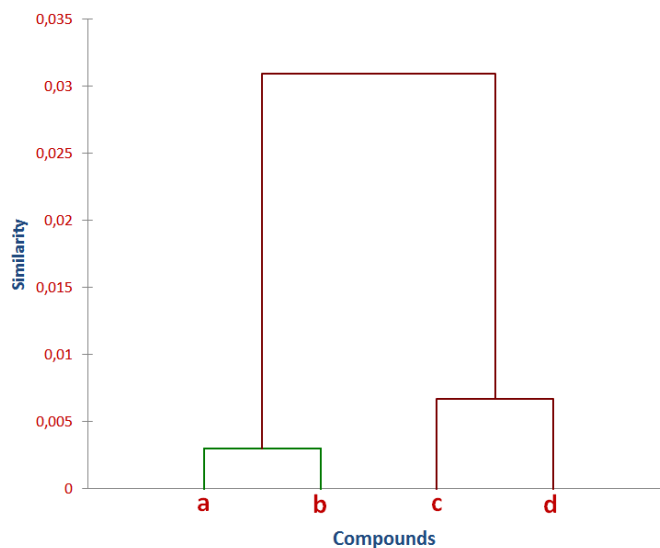


Fig.-6: Dendrogram obtained for *p*-Aminophenyl tetrathiafulvalenes studied

### CONCLUSION

In the present work we have calculated the geometrical parameters and frontier orbitals and it found that these theoretical results are in good agreement with the experimental data. Information about the charge density distribution and site of chemical activity of the molecule has been obtained by reactivity descriptors and MESP surface. Theoretical results from reactivity descriptors show that nitrogen N is more reactive site for nucleophilic and free radical attacks in compounds (a-d) and the more reactive site for electrophilic attack is 22C for compound (a), 14C for compound (b), 16C for compound (c) and 7C for compound (d). Chemometric methods shows the separation between more active (a, b) and less active compounds (c, d).

### ACKNOWLEDGMENTS

This work was generously supported by the (General Directorate for Scientific Research and Technological Development, DGRS-DT) and Algerian Ministry of Scientific Research.

### REFERENCES

1. G. Raja, K. Saravanan and S. Sivakumar, *Rasayan J. Chem.* **8** (1), 1 (2015).
2. G. Raja, K. Saravanan and S. Sivakumar, *Rasayan J. Chem.* **8** (1), 37 (2015).
3. P. Hohenberg and W. Kohn, *Phys. Rev. B*, **136**, 864 (1964).
4. W. Kohn and L.J. Sham, *Phys. Rev. A*, **140**, 1133 (1965).
5. P. Geerlings, F. De Proft and W. Langenaeker, *Chem. Rev.*, **103**, 1793 (2003).
6. T. Mineva and T. Heine, *J. Phys. Chem. A*, **108**, 11086 (2004).
7. G. Molteni and A. Ponti, *J. Chem. Eur.*, **9**, 2770 (2003).
8. S. Shetty, R. Kar, D.G. Kanhere and S. Pal, *J. Phys. Chem. A*, **110**, 252 (2006).
9. H.M. Nguyen, J. Peeters and M.T Nguyen, *J. Phys. Chem. A*, **108**, 484 (2004).
10. M.L. Romero and F. Mendez, *J. Phys. Chem. A*, **107**, 5874 (2003).
11. P.K. Chattaraj and B. Maiti, *J. Phys. Chem. A*, **105**, 169 (2001).
12. S. Saha and R.K. Roy, *Annu. Rep. Prog. Chem. Sect. C: Phys. Chem.*, **106**, 118 (2010).

13. S. Saha and R.K. Roy, *J. Phys. Chem. B*, **111**, 9664 (2007).
14. P.K. Chattaraj, U. Sarkar and D.R. Roy, *Chem. Rev*, **106**, 2065 (2006).
15. H.S. De, S. Krishnamurty and S. Pal, *J. Phys. Chem. C*, **113**, 7101 (2009).
16. G. Roos, P. Geerlings and J. Messens, *J. Phys. Chem. B*, **113**, 13465 (2009).
17. K. Fukui, Y. Yonezawa and H. Shingu, *J. Chem. Phys*, **20**, 722 (1952).
18. R.G. Parr and W. Yang, *J. Am. Chem. Soc*, **106**, 4049 (1984).
19. P.W. Ayers and M. Levy, *Chem. Acc*, **103**, 353 (2000).
20. M.J. Frisch, G.W. Trucks, H.B. Schlegel, G.E. Scuseria, M.A. Robb, J.R. Cheeseman, G. Scalmani, V. Barone, B. Mennucci, G.A. Petersson and al. Gaussian 09, Revision C.01; Gaussian Inc.: Wallingford, CT, USA (2010).
21. H.B. Schlegel, *J. Comput. Chem*, **3**, 214 (1982).
22. R. Ditchfield, W.J. Hehre, J.A. Pople, *J. Chem. Phys*, **54**, 724 (1971).
23. R. Dennington, T. Keith and J. Millam, GaussView, Version 5, Semichem Inc., Shawnee Mission, KS (2009).
24. A.D. Becke, *J. Chem. Phys*, **98**, 5648 (1993).
25. T. Koopmans, *Physica*, 1104 (1993).
26. T. Abbaz, A. Bendjeddou, N. Nait Said, R. Khammar, D. Bouchouk, S. Bouacherine, N. Sedira, S. Maache, A.k. Gouasmia, R. Rehamnia, M. Dekhici and D. Villemin, *J. Chem. Pharm. Res*, **6**, 1385 (2014).
27. A.T. Bruni and V.B. Pereira, Quantum Chemistry and Chemometrics Applied to Conformational Analysis, Quantum Chemistry - Molecules for Innovations, Tomofumi Tada (Ed.), ISBN: 978-953-51-0372-1 (2012).
28. N.L. Allinger, Molecular Structure Understanding Steric and Electronic Effects from Molecular Mechanics, John Wiley & Sons (2007).
29. C.S. Tsai, Biomacromolecules Introduction to Structure, Function and Informatics, John Wiley & Sons (2007).
30. R.M. Mohareb, E. El-Arabe and K.A. El-Sharkawy, *Sci. Pharm*, **77**, 355 (2009).
31. S.W. Xia, X. Xu, Y.L. Sun, Y.L. Fan, Y.H. Fan, C.F. Bi, D.M. Zhang and L.R. Yang, *Chin. J. Struct. Chem*, **25**, 849 (2006).
32. A.H. Pandith and N. Islam, *Int. J. Quant. Chem*, **113**, 830 (2013).
33. W. Yang and R.G. Parr, *Proc. Natl. Acad. Sci*, **82**, 6723 (1985).
34. C. Lee, W. Yang and G.R. Parr, *Phys. Rev. B*, **37**, 785 (1988).
35. R.G. Parr, L. Szentpaly and S. Liu, *J. Am. Chem. Soc*, **121**, 1922 (1999).
36. P.K. Chattaraj, U.D. Sarkar and D.R. Roy, *Chem. Rev*, **106**, 2065 (2006).
37. P.K. Chattaraj and D.R. Roy, *Chem. Rev*, **107**, 46 (2007).
38. L.V. Parr, *J. Am. Chem. Soc*, **121**, 1922 (1999).
39. J. Sponer and P. Hobza, *Int. J. Quantum Chem*, **57**, 959 (1996).
40. R.G. Parr and R.G. Pearson, *J. Am. Chem. Soc*, **105**, 7512 (1983).
41. R.G. Parr, L.V. Szentpaly and S. Liu, *J. Am. Chem. Soc*, **121**, 1922 (1999).
42. P.K. Chattaraj, H. Lee and R.G. Parr, *J. Am. Chem. Soc*, **113**, 1855 (1991).
43. P.K. Chattaraj and S. Giri, *J. Phys. Chem. A*, **111**, 11116 (2007).

[RJC-1385/2016]